

Universal Adversarial Examples and Perturbations for Quantum Classifiers

Weiyan Gong¹ and Dong-Ling Deng^{1,2,*}

¹Center for Quantum Information, IIIS, Tsinghua University, Beijing 100084, People's Republic of China

²Shanghai Qi Zhi Institute, 41th Floor, AI Tower, No. 701 Yunjin Road, Xuhui District, Shanghai 200232, China

Quantum machine learning explores the interplay between machine learning and quantum physics, which may lead to unprecedented perspectives for both fields. In fact, recent works have shown strong evidences that quantum computers could outperform classical computers in solving certain notable machine learning tasks. Yet, quantum learning systems may also suffer from the vulnerability problem: adding a tiny carefully-crafted perturbation to the legitimate input data would cause the systems to make incorrect predictions at a notably high confidence level. In this paper, we study the universality of adversarial examples and perturbations for quantum classifiers. Through concrete examples involving classifications of real-life images and quantum phases of matter, we show that there exist universal adversarial examples that can fool a set of different quantum classifiers. We prove that for a set of k classifiers with each receiving input data of n qubits, an $O(\frac{\ln k}{2^n})$ increase of the perturbation strength is enough to ensure a moderate universal adversarial risk. In addition, for a given quantum classifier we show that there exist universal adversarial perturbations, which can be added to different legitimate samples and make them to be adversarial examples for the classifier. Our results reveal the universality perspective of adversarial attacks for quantum machine learning systems, which would be crucial for practical applications of both near-term and future quantum technologies in solving machine learning problems.

Machine learning, or more broadly artificial intelligence, has achieved dramatic success over the past decade [1, 2] and a number of problems that were notoriously challenging, such as playing the game of Go [3, 4] or predicting protein structures [5], have been cracked recently. In parallel, the field of quantum computing [6] has also made remarkable progress in recent years, with the experimental demonstration of quantum supremacy marked as the latest milestone [7, 8]. The marriage of these two fast-growing fields gives birth to a new research frontier—quantum machine learning [9–11]. On the one hand, machine learning tools and techniques can be exploited to solve difficult problems in quantum science, such as quantum many-body problems [12], state tomography [13], topological quantum compiling [14], structural and electronic transitions in disordered materials [15], non-locality detection [16], and classification of different phases of matter and phase transitions [17–26]. On the other hand, new quantum algorithms running on quantum devices also possess the unparalleled potentials to enhance, speed up, or innovate machine learning [27–34]. Notable examples along this direction include the Harrow-Hassidim-Lloyd algorithm [27], quantum principal component analysis [28], quantum generative models [31–33], and quantum support vector machines [35], etc. Without a doubt, the interaction between machine learning and quantum physics will benefit both fields [11].

In classical machine learning, it has been shown that classifiers based on deep neural networks are rather vulnerable in adversarial scenarios [36–38]: adding a tiny amount of carefully-crafted noises, which are even imperceptible to human eyes and ineffective to traditional methods, into the original legitimate data may cause the classifiers to make incorrect predictions at a notably high confidence level. A celebrated example that clearly showcases the vulnerability of deep learning was observed by Szegedy *et al.* [39], where an image of a panda will be misclassified as a gibbon after adding an imperceptible amount of noises. The crafted input samples

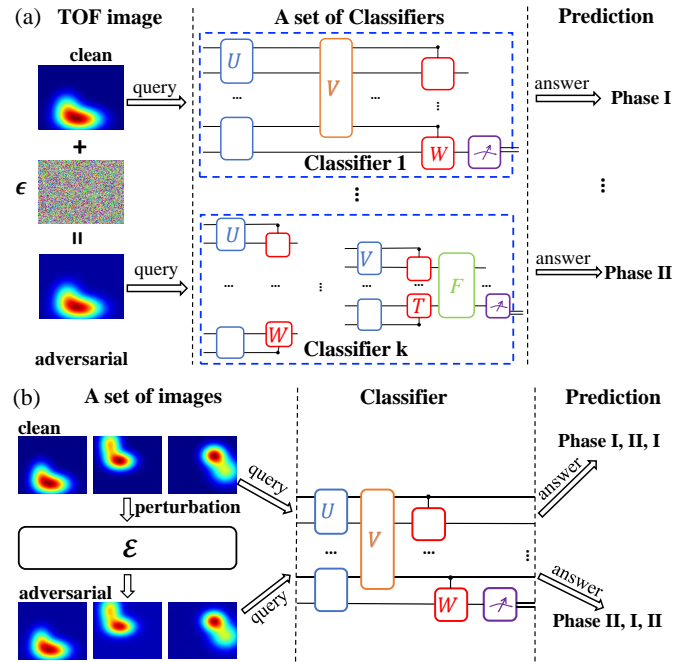


FIG. 1: A schematic illustration of universal adversarial examples and perturbations. (a) Universal adversarial examples: a set of quantum classifiers can be trained to assign phase labels to different time-of-flight images, which can be obtained directly in cold atom experiments. Adding a small amount of carefully crafted noise to a certain image could make it become a universal adversarial example, namely the new crafted image could deceive all the classifiers in the set. (b) Universal adversarial perturbations: adding the same carefully-constructed noise to a set of images could make them all become adversarial examples for a given quantum classifier.

that would deceive the classifiers are called adversarial examples. Now, it is widely believed that the existence of adversarial examples is ubiquitous in classical machine learning—almost all learning models suffer from adversarial attacks, re-

ardless of the input data types and the details of the neural networks [36–38]. More recently, the vulnerability of quantum classifiers has also been studied, sparking a new research frontier of quantum adversarial machine learning [40–45]. In particular, Ref. [40] explored different adversarial scenarios in the context of quantum machine learning and have demonstrated that, with a wide range of concrete examples, quantum classifiers are likewise highly vulnerable to crafted adversarial examples. This emergent research direction is growing rapidly, attracting more and more attentions across communities. Yet, it is still in its infancy and many important issues remain unexplored.

In this paper, we consider such an issue concerning the universality of adversarial examples and perturbations for quantum classifiers. We ask two questions: (i) whether there exist universal adversarial examples that could fool a set of different quantum classifiers? (ii) whether there exist universal adversarial perturbations, which when added to different legitimate input samples could make them become adversarial examples for a given quantum classifier? Based on extensive numerical simulations and analytical analysis, we give affirmative answers to both questions. For (i), we prove that, by exploring the concentration of measure phenomenon [46], an $O(\frac{\ln k}{2^n})$ increase of the perturbation strength is enough to ensure a moderate universal adversarial risk for a set of k quantum classifiers with each receiving input data of n qubits; For (ii), we prove that, based on the quantum no free lunch theorem [47, 48], the universal adversarial risk is bounded from both below and above and approaches unit exponentially fast as the number of qubits for the quantum classifier increase. We carry out extensive numerical simulations on concrete examples involving classifications of real-life images and quantum phases of matter to demonstrate how to obtain universal adversarial examples and perturbations in practice.

Universal adversarial examples.—To begin with, we first introduce some concepts and notations. Consider a classification task in the setting of supervised learning, where we assign a label $s \in S$ to an input data sample $\rho \in \mathcal{H}$, with S being a countable label set and \mathcal{H} the set of all possible samples. The training set is denoted as $\mathcal{S}_N = \{(\rho_1, s_1), \dots, (\rho_N, s_N)\}$, where $\rho_i \in \mathcal{H}$, $s_i \in S$, and N is the size of the training set. Essentially, the task of classification is to learn a function (called a hypothesis function) $h : \mathcal{H} \rightarrow S$, which for a given input $\rho \in \mathcal{H}$ outputs a label s [49]. We denote the *ground truth* function as $t : \mathcal{H} \rightarrow S$, which gives the true classification for any $\rho \in \mathcal{H}$. For the purpose in this paper, we suppose that after the training process the hypothesis function match the ground truth function on the training set, namely $h(\rho) = t(\rho), \forall \rho \in \mathcal{S}_N$. We consider a set of k quantum classifiers $\mathcal{C}_1, \dots, \mathcal{C}_k$ with corresponding hypothesis functions h_i ($i = 1, \dots, k$) and introduce the following definitions to formalize our results.

Definition 1. We suppose the input sample ρ is chosen from \mathcal{H} according to a probability measure μ and $\mu(\mathcal{H}) = 1$. For h_i , we define $\mathcal{E}_i = \{\rho \in \mathcal{H} | h_i(\rho) \neq t(\rho)\}$ as the misclassified set, and the *risk* for \mathcal{C}_i is denoted as $\mu(\mathcal{E}_i)$.

Definition 2. Consider a metric over \mathcal{H} with the distance measure denoted as $D(\cdot)$. Then the ϵ -expansion of a subset $\mathcal{H}' \subseteq \mathcal{H}$ is defined as: $\mathcal{H}'_\epsilon = \{\rho | D_{\min}(\rho, \mathcal{H}') \leq \epsilon\}$, where $D_{\min}(\rho, \mathcal{H}')$ denotes the minimum distance between ρ and any $\rho' \in \mathcal{H}'$. In the context of adversarial learning, a perturbation within distance ϵ added to the legitimate input sample $\rho \in \mathcal{E}_{i,\epsilon} = \{\rho' | D_{\min}(\rho', \mathcal{E}_i)\}$ can shift it to some misclassified one for the quantum classifier \mathcal{C}_i . Hence, we define the adversarial risk for \mathcal{C}_i as $\mu(\mathcal{E}_{i,\epsilon})$. Similarly, the universal adversarial risk for a set of k quantum classifiers is defined as $R = \mu(\mathcal{E}_\epsilon)$, where $\mathcal{E}_\epsilon = \cap_{i=1}^k \mathcal{E}_{i,\epsilon}$ denotes the set of universal adversarial samples.

For technique simplicity and convenience, we focus on $\mathcal{H} = SU(d)$ (the special unitary group) with the Hilbert-Schmidt distance $D_{\text{HS}}(\rho, \rho')$ and Haar probability measure [50]. We mention that the input data ρ can be either classical or quantum in general. We treat both cases on the same footing since we can always encode the classical data into quantum states. We also note that any input state could be prepared by acting a unitary transformation on a certain initial state (e.g., the $|00 \dots 0\rangle$ state) and hence the classification of quantum states is in some sense equivalent to the classification of unitary transformations. Now, we are ready to present one of our main results.

Theorem 1. Consider a set of k quantum classifiers \mathcal{C}_i , $i = 1, \dots, k$ and let $\mu(\mathcal{E})_{\min}$ be the minimum risk among $\mu(\mathcal{E}_i)$. Suppose $\rho \in SU(d)$ and a perturbation $\rho \rightarrow \rho'$ occurs with $D_{\text{HS}}(\rho, \rho') \leq \epsilon$, then we can ensure that the universal adversarial risk is bounded below by R_0 if

$$\epsilon^2 \geq \frac{4}{d} \ln \left[\frac{2k}{\mu(\mathcal{E})_{\min}(1 - R_0)} \right]. \quad (1)$$

Proof. We give the main idea and intuition here. The full proof is a bit technically involved and thus left to the Supplementary Materials [51]. The first step is to prove that for a single quantum classifier \mathcal{C}_i , we can ensure that its adversarial risk is bounded below by $R_{0,i}$ if $\epsilon^2 \geq \frac{4}{d} \ln \left[\frac{2}{\mu(\mathcal{E}_i)(1 - R_{0,i})} \right]$. This can be done by exploring the concentration of the measure phenomenon for $SU(d)$ equipped with the Haar measure and Hilbert-Schmidt metric [41, 52]. Next, we use the De Morgan's laws in set theory to deduce that $\mu(\mathcal{E}_\epsilon) \geq 1 - k + \sum_{i=1}^k \mu(\mathcal{E}_i)$. In the last step, we choose $R_{0,i} = \frac{k-1+R_0}{k}$ and replace $\mu(\mathcal{E}_i)$ by $\mu(\mathcal{E})_{\min}$ to increase ϵ a little bit for each \mathcal{C}_i . This leads to Eq. (1) and complete the proof.

The above theorem implies that for a set of k quantum classifiers with each receiving input data of n qubits (thus $d = 2^n$), an $O(\frac{\ln k}{2^n})$ increase of the perturbation strength would guarantee a moderate universal adversarial risk lower bounded by R_0 . As n increases, the lower bound of ϵ approaches zero exponentially. In other words, an exponentially small adversarial perturbation could result in universal adversarial examples that can deceive all k classifiers with constant probability. This is a fundamental feature of quantum classifiers in high dimensional Hilbert space due to the concentration of the measure phenomenon, independent of their specific

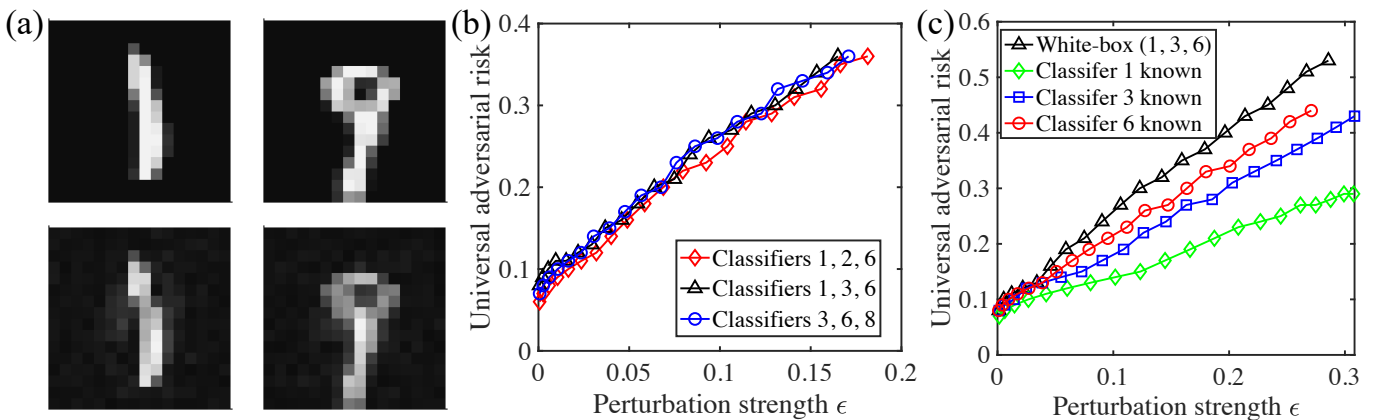


FIG. 2: Numerical results on universal adversarial examples. In this figure, the adversarial examples are obtained through the qBIM algorithm with step size $\alpha = 0.02$. (a) The clean and the corresponding universal adversarial handwritten digit images that can deceive all eight quantum classifiers. (b) The universal adversarial risk as a function of the perturbation strength ϵ for different subsets of the classifiers in classifying the ground states of the 1D transverse field Ising model. Here, we consider the white-box attack scenario and the universal adversarial risk is defined as the ratio of test samples that deceive all three classifiers in each subset. (c) Results for attacking a subset of classifiers consisting of classifiers 1, 3, and 6, in a white-box black-box hybrid setting. Here, we assume that only one of the classifiers is known to the attacker, and for comparison the black curve with triangles plots the result for the white-box attack case. For more details, see the Supplementary Material [51].

structures and the input datasets.

Although the above theorem indicates the existence of universal adversarial examples in theory, it is still unclear how to obtain these universal examples in practice. To deal with this issue, in the following we provide concrete examples involving classifications of hand-writing digit images and quantum phases with extensive numerical simulations. We mention that, in the classical adversarial machine learning literature, universal adversarial examples have also been shown to exist in real applications. For instance, in Ref. [53] it is shown that an attacker can fool (such as dodging or impersonation) a number of the state-of-the-art face-recognition systems by simply wearing a pair of carefully-crafted eyeglasses. For our purpose, we consider a set of eight quantum classifiers with different structures, labeled by numbers from 1 to 8. The classifiers 1 and 2 are two quantum convolutional neural networks (QCNNs) [54] and the classifiers 3–8 are other typical multi-layer variational quantum circuits with depths from five through ten. The detailed descriptions of these quantum classifiers are given in the Supplementary Materials [51].

The first example we consider is the classification of handwritten-digit images in the MNIST dataset [55], which is a prototypical testbed for benchmarking various machine learning scenarios. This dataset consists of gray-scale images of handwritten digits from 0 through 9, with each of them contains 28×28 pixels. We reduce the size of the images to 16×16 , so that we can simulate the learning and attacking process of the quantum classifiers with moderate classical computational resources. We use amplitude encoding to map the input images into quantum states and the cross-entropy as the loss function for training and adversarial attacking. After training, we use the quantum-adapted basic iterative method (qBIM) [56] to obtain the adversarial examples. The details

of the training and adversarial attacking process are provided in the Supplementary Materials [51]. In Fig.2 (a), we display two universal adversarial examples for digits 1 and 9, which can deceive *all* eight quantum classifiers at a high-confidence level. Notably, these universal adversarial examples only differ from the original legitimate ones slightly and they can be easily identified by human eyes. In fact, the fidelity between the adversarial and legitimate samples is about 96%, which is fairly high given that the Hilbert dimension involved is not very large ($d = 256$ for this case).

The above discussion concerns the vulnerability of quantum classifiers in classifying classical data (images). Yet, unlike classical classifiers that can only take classical data as input, quantum classifiers can also directly classify quantum data (states) produced by quantum devices. To demonstrate the existence of universal adversarial examples in such a scenario, we consider classifying the ground state of the one-dimensional (1D) transverse field Ising model:

$$H_{\text{Ising}} = - \sum_{i=1}^{L-1} \sigma_i^z \sigma_{i+1}^z - J_x \sum_{i=1}^L \sigma_i^x, \quad (2)$$

where J_x denotes the strength of the transverse field and σ_i^x and σ_i^z are the Pauli matrices for the i -th spin. This Hamiltonian maps to free fermions via Jordan-Wigner transformation [57] and is exactly solvable. Its ground state features a quantum phase transition at $J_x = 1$, between ferromagnetic phase with $J_x > 1$ and paramagnetic phase with $0 < J_x < 1$. We consider classifying these two different phases by the eight quantum classifiers mentioned above, with the ground state as input data. We sample the Hamiltonian with varying J_x from 0 to 2 and compute their corresponding ground states. These quantum states with their corresponding labels form the

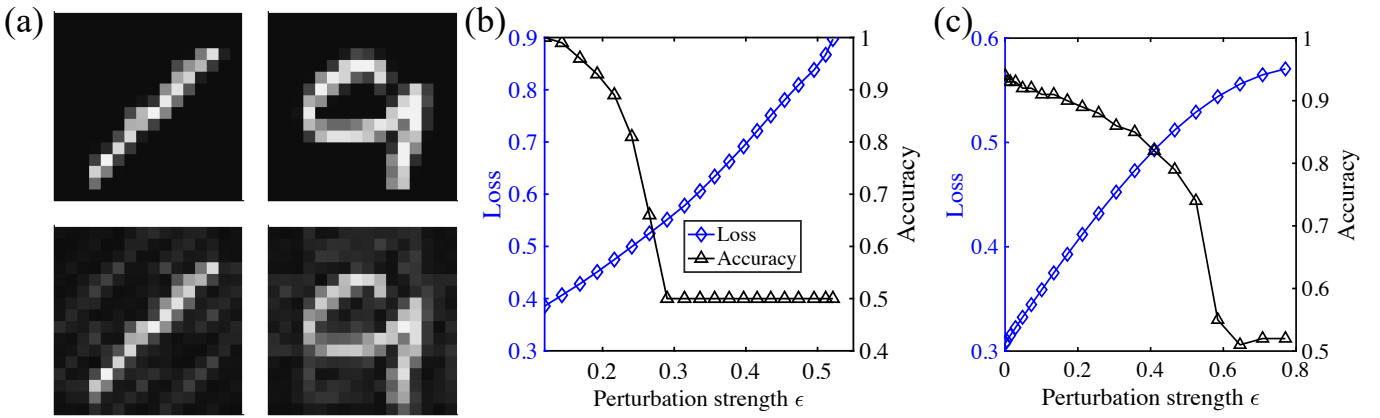


FIG. 3: Numerical results on universal adversarial perturbations. Similar to Fig. 2, in this figure the adversarial perturbations are also obtained by the qBIM algorithm with step size $\alpha = 0.02$. (a) The clean and corresponding adversarial examples that can fool the quantum classifier 2, which is a quantum convolutional neural network. These two adversarial images (bottom) are obtained by adding the same perturbation to the original legitimate ones. (b) The loss and accuracy as functions of the perturbation strength ϵ for the classifier 2 in classifying the ground states of H_{sing} . (c) A similar result for the classifier 8. Throughout this figure, the white-box attack is considered. For more details, see the Supplementary Material [51].

dataset required [51].

In Fig. 2(b), we consider three subsets of quantum classifiers in a white-box attack setting (namely the attacker has full information about the learned model and the learning algorithm). We find that universal adversarial examples indeed exist for classifying quantum states, regardless of the internal structures of the classifiers. As the perturbation strength ϵ increases, the universal adversarial risk increases roughly linearly with ϵ . With a perturbation strength $\epsilon = 0.18$, we find that 37% of the test samples could become universal adversarial examples for each subset of the classifiers. In Fig. 2(c), we consider a white-box black-box hybrid scenario, where the attacker knows only the full information about one classifier in the subset and does not have any information about the rest ones. The motivation of this consideration is to study the transferability of universal adversarial examples. From Fig. 2(c), we find that even with limited partial information, the adversary is still able to create universal adversarial examples, indicating a notable transferability property of these examples. The universal adversarial risk also increases linearly with ϵ , but it is noticeably smaller than that for the white-box case. This is consistent with the intuition that the more information the attacker has the easier to create adversarial examples.

Universal adversarial perturbations.—In the above discussion, we demonstrate, with both theoretical analysis and numerical simulations, that there exist universal adversarial examples that could deceive a set of distinct quantum classifiers. We now turn to the second question and show that there exist universal adversarial perturbations that can be added to different legitimate samples and make them adversarial to a given quantum classifier \mathcal{C} . Without loss of generality, we may consider a unitary perturbation $\hat{\epsilon} : \mathcal{H} \rightarrow \mathcal{H}$ as means of adversarial attack for all input samples. We denote the misclassified set as $\mathcal{E} = \{\rho \in \mathcal{H} | h(\rho) \neq t(\rho)\}$ and consequently the unitary

adversarial set as $\mathcal{E}_{\hat{\epsilon}} = \{\hat{\epsilon}^{-1}(\rho) | \rho \in \mathcal{E}\}$.

Theorem 2. For an adversarial perturbation with unitary operator $\hat{\epsilon}$ and n samples ρ_1, \dots, ρ_n chosen from \mathcal{H} according to the Haar measure, the performance of the quantum classifier \mathcal{C} with $\hat{\epsilon}(\rho_1), \dots, \hat{\epsilon}(\rho_n)$ as input samples is bounded by:

$$|R_E - \mu(\mathcal{E})| \leq \sqrt{\frac{1}{2n} \ln\left(\frac{2}{\delta}\right)} \quad (3)$$

with probability at least $1 - \delta$ ($0 < \delta < 1$). Here R_E is the empirical error rate defined as the ratio of the misclassified samples and $\mu(\mathcal{E})$ is the risk for \mathcal{C} . In addition, the expectation of the risk over all ground truth t and training set \mathcal{S}_N is bounded below by:

$$\mathbb{E}_t[\mathbb{E}_{\mathcal{S}_N}[\mu(\mathcal{E})]] \geq 1 - \frac{d'}{d(d+1)}(N^2 + d + 1), \quad (4)$$

where $d = \dim(\mathcal{H})$ is the dimension of the input data and $d' = |S|$ is the number of output labels.

Proof. We only sketch the major steps here and leave the details of the full proof to the Supplementary Materials [51]. Noting that unitary transformations are invertible, the unitary perturbation operator $\hat{\epsilon}$ will transfer samples in $\mathcal{E}_{\hat{\epsilon}}$ into the misclassified set \mathcal{E} , and we can therefore deduce that $\mu(\mathcal{E}) = \mu(\mathcal{E}_{\hat{\epsilon}})$. Then from the definition of $\mu(\mathcal{E})$, the Ineq. (3) follows straightforwardly by applying the Hoeffding's inequality [58]. The derivation of the Ineq. (4) relies on the recent works about reformulation of the no free lunch theorem [59] in the context of quantum machine learning [47, 48] (see the Supplementary Materials for details).

This theorem indicates that in the limit $d \rightarrow \infty$, the expectation of the risk for a general quantum classifier goes to unit, independent of its structure and the training algorithm. For a fixed d , the lower bound of such an expectation decreases as the number of the output labels or the size of the training

set increase. Adding an identical adversarial unitary perturbation to all possible data samples will not increase the risk on average. However, it is still possible for such a perturbation to increase the ratio of misclassified samples for a given finite set of n original samples. In the following, we carry out numerical simulations and show how to obtain the universal adversarial perturbations in classifying images of handwritten digits and the ground states of the 1D transverse field Ising model. To implement the unitary perturbation $\hat{\epsilon}$, we add an additional variational layer before the original quantum classifiers. After training, we fix the variational parameters of the given classifier \mathcal{C} and optimize the parameters of the perturbation layer through the qBIM algorithm to maximize the loss function for a given set of n original samples [51].

The major results are shown in Fig. 3. In Fig. 3(a), we display two adversarial examples for digits 1 and 9, which are obtained by adding the same unitary perturbation to the original images and can fool the classifier 2 (one of the QCNN classifiers mentioned above). We mention that the fidelity between the original and crafted images is relatively small (about 78%) compared with the examples given in Fig. 2(a), but the crafted images remain easily identifiable by human eyes. In Fig. 3(b), we consider adding the same unitary perturbation to all the test samples of the ground states of H_{Ising} in a white-box attack setting for classifier 2. From this figure, it is clear that the accuracy drops rapidly at first as we increase the perturbation strength, and then maintains at a fixed finite value (about 0.5). This is consistent with the Ineq.(3) that R_E has an upper bound around $\mu(\mathcal{E})$. We mention that the loss keeps increasing as the perturbation strength increases, even in the region where the accuracy becomes flattened. This counterintuitive behavior is due to the fact that the loss function (cross-entropy) is continuous, whereas the accuracy is defined by the ratio of correctly classified samples whose labels are assigned according to the largest output probability. Fig. 3(c) shows similar results as in Fig. 3(b), but for a different quantum classifier (i.e., the classifier 10 mentioned above).

We remark that in our numerical simulations the Hilbert dimension involved is not very large due to limited classical computational resources. Consequently, a larger perturbation is needed to create the adversarial examples. As in Fig. 3(a), the perturbation is perceptible to human eyes. However, this is by no means a pitfall in principle and can be circumvented by simulating larger quantum classifiers. As noisy intermediate-scale quantum devices [60] now become available in laboratories [7], this may also be resolved by running the protocol in real quantum devices. In addition, although we only focus on two-category classifications for simplicity in this paper, the extension to multi-category classifications and other adversarial scenarios is straightforward.

Discussion and conclusion.—This work only reveals the tip of the iceberg in the fledgling field of quantum adversarial machine learning. Many important questions remain unexplored and demand further investigations. First, this work shows that the existence of universal adversarial examples is a fundamental feature of quantum learning in high-dimensional space in

general. However, for a given learning task, the legitimate samples may only occupy a tiny subspace of the whole Hilbert space. This brings about the possibility of defending against adversarial attacks. In practice, how to develop appropriate countermeasures feasible in experiments to strengthen the reliability of quantum classifiers still remains unclear. In addition, unsupervised and reinforcement learning approaches may also suffer from the vulnerability problem [61]. Yet, in practice it is often more challenging to obtain adversarial examples in these scenarios. The study of quantum adversarial learning in the unsupervised or reinforcement setting is still lacking. In particular, how to obtain adversarial examples and perturbations and study their universality properties for quantum unsupervised or reinforcement learning remains entirely unexplored and is well worth future investigations. Finally, it would be interesting and important to carry out an experiment to demonstrate the existence of universal adversarial examples and perturbations. This would be a crucial step toward practical applications of quantum technologies in artificial intelligence in the future, especially for these applications in safety and security-critical environments, such as self-driving cars, malware detection, biometric authentication, and medical diagnostics [62].

In summary, we have studied the universality of adversarial examples and perturbations for quantum classifiers. We proved two relevant theorems: one states that an $O(\frac{\ln k}{2^n})$ increase of the perturbation strength is already sufficient to ensure a moderate universal adversarial risk for a set of k quantum classifiers, and the other asserts that, for a general quantum classifier, the empirical error rate is bounded from both below and above and approaches to unit exponentially fast as the size of the classifier increases. We carried out extensive numerical simulations on concrete examples to demonstrate the existence of universal adversarial examples and perturbations for quantum classifiers in reality. Our results uncover a new aspect about the vulnerability of quantum machine learning systems, which would provide valuable guidance for practical applications of quantum classifiers based on both near-term and future quantum technologies.

We thank Sirui Lu, Weikang Li, Xun Gao, Si Jiang, Wenjie Jiang and Nana Liu for helpful discussions. This work is supported by the start-up fund from Tsinghua University (Grant. No. 53330300320), the National Natural Science Foundation of China (Grant. No. 12075128), and the Shanghai Qi Zhi Institute.

* Electronic address: dldeng@tsinghua.edu.cn

- [1] Y. LeCun, Y. Bengio, and G. Hinton, “Deep learning,” *Nature* **521**, 436 (2015).
- [2] M. Jordan and T. Mitchell, “Machine learning: Trends, perspectives, and prospects,” *Science* **349**, 255 (2015).
- [3] D. Silver, A. Huang, C. J. Maddison, A. Guez, L. Sifre, G. Van Den Driessche, J. Schrittwieser, I. Antonoglou, V. Panneershelvam, M. Lanctot, *et al.*, “Mastering the game of go with

- deep neural networks and tree search,” *nature* **529**, 484 (2016).
- [4] D. Silver, J. Schrittwieser, K. Simonyan, I. Antonoglou, A. Huang, A. Guez, T. Hubert, L. Baker, M. Lai, A. Bolton, *et al.*, “Mastering the game of go without human knowledge,” *Nature* **550**, 354 (2017).
- [5] A. W. Senior, R. Evans, J. Jumper, J. Kirkpatrick, L. Sifre, T. Green, C. Qin, A. Žídek, A. W. R. Nelson, A. Bridgland, H. Penedones, S. Petersen, K. Simonyan, S. Crossan, P. Kohli, D. T. Jones, D. Silver, K. Kavukcuoglu, and D. Hassabis, “Improved protein structure prediction using potentials from deep learning,” *Nature* **577**, 706 (2020).
- [6] M. A. Nielsen and I. L. Chuang, *Quantum Computation and Quantum Information* (Cambridge University Press, Cambridge, 2010).
- [7] F. Arute, K. Arya, R. Babbush, D. Bacon, J. C. Bardin, R. Barends, R. Biswas, S. Boixo, F. G. Brandao, D. A. Buell, *et al.*, “Quantum supremacy using a programmable superconducting processor,” *Nature* **574**, 505 (2019).
- [8] H.-S. Zhong, H. Wang, Y.-H. Deng, M.-C. Chen, L.-C. Peng, Y.-H. Luo, J. Qin, D. Wu, X. Ding, Y. Hu, *et al.*, “Quantum computational advantage using photons,” *Science* **370**, 1460 (2020).
- [9] J. Biamonte, P. Wittek, N. Pancotti, P. Rebentrost, N. Wiebe, and S. Lloyd, “Quantum machine learning,” *Nature* **549**, 195 (2017).
- [10] V. Dunjko and H. J. Briegel, “Machine learning & artificial intelligence in the quantum domain: a review of recent progress,” *Rep. Prog. Phys.* **81**, 074001 (2018).
- [11] S. D. Sarma, D.-L. Deng, and L.-M. Duan, “Machine learning meets quantum physics,” *Physics Today* **72**, 48 (2019).
- [12] G. Carleo and M. Troyer, “Solving the quantum many-body problem with artificial neural networks,” *Science* **355**, 602 (2017).
- [13] G. Torlai, G. Mazzola, J. Carrasquilla, M. Troyer, R. Melko, and G. Carleo, “Neural-network quantum state tomography,” *Nat. Phys.* , 1 (2018).
- [14] Y.-H. Zhang, P.-L. Zheng, Y. Zhang, and D.-L. Deng, “Topological Quantum Compiling with Reinforcement Learning,” *Phys. Rev. Lett.* **125**, 170501 (2020).
- [15] V. L. Deringer, N. Bernstein, G. Csányi, C. B. Mahmoud, M. Ceriotti, M. Wilson, D. A. Drabold, and S. R. Elliott, “Origins of structural and electronic transitions in disordered silicon,” *Nature* **589**, 59 (2021).
- [16] D.-L. Deng, “Machine learning detection of bell nonlocality in quantum many-body systems,” *Phys. Rev. Lett.* **120**, 240402 (2018).
- [17] Y. Zhang and E.-A. Kim, “Quantum Loop Topography for Machine Learning,” *Phys. Rev. Lett.* **118**, 216401 (2017).
- [18] J. Carrasquilla and R. G. Melko, “Machine learning phases of matter,” *Nat. Phys.* **13**, 431 (2017).
- [19] E. P. L. van Nieuwenburg, Y.-H. Liu, and S. D. Huber, “Learning phase transitions by confusion,” *Nat. Phys.* **13**, 435 (2017).
- [20] L. Wang, “Discovering phase transitions with unsupervised learning,” *Phys. Rev. B* **94**, 195105 (2016).
- [21] P. Broecker, J. Carrasquilla, R. G. Melko, and S. Trebst, “Machine learning quantum phases of matter beyond the fermion sign problem,” *Sci. Rep.* **7** (2017), 10.1038/s41598-017-09098-0.
- [22] K. Ch’ng, J. Carrasquilla, R. G. Melko, and E. Khatami, “Machine learning phases of strongly correlated fermions,” *Phys. Rev. X* **7**, 031038 (2017).
- [23] S. J. Wetzel, “Unsupervised learning of phase transitions: From principal component analysis to variational autoencoders,” *Phys. Rev. E* **96**, 022140 (2017).
- [24] W. Hu, R. R. P. Singh, and R. T. Scalettar, “Discovering phases, phase transitions, and crossovers through unsupervised machine learning: A critical examination,” *Phys. Rev. E* **95**, 062122 (2017).
- [25] Y. Zhang, A. Mesaros, K. Fujita, S. Ekins, M. Hamidian, K. Ch’ng, H. Eisaki, S. Uchida, J. S. Davis, E. Khatami, *et al.*, “Machine learning in electronic-quantum-matter imaging experiments,” *Nature* **570**, 484 (2019).
- [26] W. Lian, S.-T. Wang, S. Lu, Y. Huang, F. Wang, X. Yuan, W. Zhang, X. Ouyang, X. Wang, X. Huang, L. He, X. Chang, D.-L. Deng, and L. Duan, “Machine learning topological phases with a solid-state quantum simulator,” *Phys. Rev. Lett.* **122**, 210503 (2019).
- [27] A. W. Harrow, A. Hassidim, and S. Lloyd, “Quantum algorithm for linear systems of equations,” *Phys. Rev. Lett.* **103**, 150502 (2009).
- [28] S. Lloyd, M. Mohseni, and P. Rebentrost, “Quantum principal component analysis,” *Nat. Phys.* **10**, 631 (2014).
- [29] V. Dunjko, J. M. Taylor, and H. J. Briegel, “Quantum-Enhanced Machine Learning,” *Phys. Rev. Lett.* **117**, 130501 (2016).
- [30] M. H. Amin, E. Andriyash, J. Rolfe, B. Kulchitsky, and R. Melko, “Quantum Boltzmann Machine,” *Phys. Rev. X* **8**, 021050 (2018).
- [31] X. Gao, Z.-Y. Zhang, and L.-M. Duan, “A quantum machine learning algorithm based on generative models,” *Science advances* **4**, eaat9004 (2018).
- [32] S. Lloyd and C. Weedbrook, “Quantum generative adversarial learning,” *Phys. Rev. Lett.* **121**, 040502 (2018).
- [33] L. Hu, S.-H. Wu, W. Cai, Y. Ma, X. Mu, Y. Xu, H. Wang, Y. Song, D.-L. Deng, C.-L. Zou, *et al.*, “Quantum generative adversarial learning in a superconducting quantum circuit,” *Science advances* **5**, eaav2761 (2019).
- [34] M. Schuld and N. Killoran, “Quantum machine learning in feature hilbert spaces,” *Phys. Rev. Lett.* **122**, 040504 (2019).
- [35] P. Rebentrost, M. Mohseni, and S. Lloyd, “Quantum support vector machine for big data classification,” *Phys. Rev. Lett.* **113**, 130503 (2014).
- [36] A. Chakraborty, M. Alam, V. Dey, A. Chattopadhyay, and D. Mukhopadhyay, “Adversarial attacks and defences: A survey,” *arXiv:1810.00069* (2018).
- [37] B. Biggio and F. Roli, “Wild patterns: Ten years after the rise of adversarial machine learning,” *Pattern Recognition* **84**, 317 (2018).
- [38] D. J. Miller, Z. Xiang, and G. Kesidis, “Adversarial learning in statistical classification: A comprehensive review of defenses against attacks,” *arXiv:1904.06292* (2019).
- [39] C. Szegedy, W. Zaremba, I. Sutskever, J. Bruna, D. Erhan, I. Goodfellow, and R. Fergus, “Intriguing properties of neural networks,” in Second International Conference on Learning Representations (ICLR, Banff, Canada, 2014) .
- [40] S. Lu, L.-M. Duan, and D.-L. Deng, “Quantum adversarial machine learning,” *Phys. Rev. Res.* **2**, 033212 (2020).
- [41] N. Liu and P. Wittek, “Vulnerability of quantum classification to adversarial perturbations,” *Phys. Rev. A* **101**, 062331 (2019).
- [42] Y. Du, M.-H. Hsieh, T. Liu, D. Tao, and N. Liu, “Quantum noise protects quantum classifiers against adversaries,” *arXiv:2003.09416* (2020).
- [43] P. Casares and M. Martin-Delgado, “A quantum active learning algorithm for sampling against adversarial attacks,” *New Journal of Physics* **22**, 073026 (2020).
- [44] J. Guan, W. Fang, and M. Ying, “Robustness verification of quantum machine learning,” *arXiv:2008.07230* (2020).

- [45] H. Liao, I. Convy, W. J. Huggins, and K. B. Whaley, “Adversarial robustness of quantum machine learning models,” [arXiv:2010.08544 \(2020\)](#).
- [46] M. Ledoux, *The concentration of measure phenomenon*, 89 (American Mathematical Soc., 2001).
- [47] K. Poland, K. Beer, and T. J. Osborne, “No free lunch for quantum machine learning,” [arXiv:2003.14103 \(2020\)](#).
- [48] K. Sharma, M. Cerezo, Z. Holmes, L. Cincio, A. Sornborger, and P. J. Coles, “Reformulation of the no-free-lunch theorem for entangled data sets,” [arXiv:2007.04900 \(2020\)](#).
- [49] I. Goodfellow, Y. Bengio, and A. Courville, *Deep learning* (MIT press, 2016).
- [50] J. G. Ratcliffe, S. Axler, and K. Ribet, *Foundations of hyperbolic manifolds*, Vol. 149 (Springer, 2006).
- [51] See Supplemental Material at [URL will be inserted by publisher] for details about the proofs of the two theorems, structures of the quantum classifiers, quantum encoding for classical data, training and attacking processes, and the algorithms for obtaining universal adversarial examples and perturbations.
- [52] S. Mahloujifar, D. I. Diochnos, and M. Mahmoody, “The curse of concentration in robust learning: Evasion and poisoning attacks from concentration of measure,” in *Proceedings of the AAAI Conference on Artificial Intelligence*, Vol. 33 (2019) pp. 4536–4543.
- [53] M. Sharif, S. Bhagavatula, L. Bauer, and M. K. Reiter, “Accessorize to a crime: Real and stealthy attacks on state-of-the-art face recognition,” in *Proceedings of the 2016 acm sigsac conference on computer and communications security* (2016) pp. 1528–1540.
- [54] I. Cong, S. Choi, and M. D. Lukin, “Quantum convolutional neural networks,” *Nat. Phys.* **15**, 1273 (2019).
- [55] *The mnist database of handwritten digits* (1998).
- [56] A. Kurakin, I. Goodfellow, and S. Bengio, “Adversarial examples in the physical world,” [arXiv:1607.02533 \(2016\)](#).
- [57] S. Sachdev, “Quantum phase transitions,” *Quantum Phase Transitions*, by Subir Sachdev, Cambridge, UK: Cambridge University Press, 2011 **1** (2011).
- [58] W. Hoeffding, “Probability inequalities for sums of bounded random variables,” *J. Am. Stat. Assoc.* **58**, 13 (1963).
- [59] S. Shalev-Shwartz and S. Ben-David, *Understanding machine learning: From theory to algorithms* (Cambridge university press, 2014).
- [60] J. Preskill, “Quantum Computing in the NISQ era and beyond,” *Quantum* **2**, 79 (2018).
- [61] Y. Vorobeychik and M. Kantarcioglu, “Adversarial machine learning,” *Synthesis Lectures on Artificial Intelligence and Machine Learning* **12**, 1 (2018).
- [62] S. G. Finlayson, J. D. Bowers, J. Ito, J. L. Zittrain, A. L. Beam, and I. S. Kohane, “Adversarial attacks on medical machine learning,” *Science* **363**, 1287 (2019).
- [63] M. Gromov and V. D. Milman, “A topological application of the isoperimetric inequality,” *Am. J. Math.* **105**, 843 (1983).
- [64] T. Giordano and V. Pestov, “Some extremely amenable groups related to operator algebras and ergodic theory,” *J. Inst. Math. Jussieu* **6**, 279 (2007).
- [65] V. D. Milman and G. Schechtman, *Asymptotic theory of finite dimensional normed spaces: Isoperimetric inequalities in riemannian manifolds*, Vol. 1200 (Springer, 2009).
- [66] E. Meckes, *Concentration of measure and the compact classical matrix groups*, edited by (unpublished) (Citeseer, 2014).
- [67] M. Oszmaniec, R. Augusiak, C. Gogolin, J. Kołodyński, A. Acín, and M. Lewenstein, “Random bosonic states for robust quantum metrology,” *Phys. Rev. X* **6**, 041044 (2016).
- [68] A. Monras, G. Sentís, and P. Wittek, “Inductive supervised quantum learning,” *Phys. Rev. Lett.* **118**, 190503 (2017).
- [69] M. Schuld, A. Bocharov, K. M. Svore, and N. Wiebe, “Circuit-centric quantum classifiers,” *Phys. Rev. A* **101**, 032308 (2020).
- [70] E. Farhi and H. Neven, “Classification with quantum neural networks on near term processors,” [arXiv:1802.06002 \(2018\)](#).
- [71] M. Schuld, M. Fingerhuth, and F. Petruccione, “Implementing a distance-based classifier with a quantum interference circuit,” *EPL (Europhysics Letters)* **119**, 60002 (2017).
- [72] K. Mitarai, M. Negoro, M. Kitagawa, and K. Fujii, “Quantum circuit learning,” *Phys. Rev. A* **98**, 032309 (2018).
- [73] J. Li, X. Yang, X. Peng, and C.-P. Sun, “Hybrid quantum-classical approach to quantum optimal control,” *Phys. Rev. Lett* **118**, 150503 (2017).
- [74] V. Havlíček, A. D. Córcoles, K. Temme, A. W. Harrow, A. Kandala, J. M. Chow, and J. M. Gambetta, “Supervised learning with quantum-enhanced feature spaces,” *Nature* **567**, 209 (2019).
- [75] D. Zhu, N. M. Linke, M. Benedetti, K. A. Landsman, N. H. Nguyen, C. H. Alderete, A. Perdomo-Ortiz, N. Korda, A. Garfoot, C. Brecque, *et al.*, “Training of quantum circuits on a hybrid quantum computer,” *Science advances* **5**, eaaw9918 (2019).
- [76] K. H. Wan, O. Dahlsten, H. Kristjánsson, R. Gardner, and M. Kim, “Quantum generalisation of feedforward neural networks,” *npj Quantum information* **3**, 1 (2017).
- [77] E. Grant, M. Benedetti, S. Cao, A. Hallam, J. Lockhart, V. Stojevic, A. G. Green, and S. Severini, “Hierarchical quantum classifiers,” *npj Quantum Information* **4**, 1 (2018).
- [78] Y. Du, M.-H. Hsieh, T. Liu, and D. Tao, “Implementable quantum classifier for nonlinear data,” [arXiv:1809.06056 \(2018\)](#).
- [79] A. Uvarov, A. Kardashin, and J. D. Biamonte, “Machine learning phase transitions with a quantum processor,” *Phys. Rev. A* **102**, 012415 (2020).
- [80] C. Blank, D. K. Park, J.-K. K. Rhee, and F. Petruccione, “Quantum classifier with tailored quantum kernel,” *npj Quantum Information* **6**, 1 (2020).
- [81] F. Tacchino, C. Macchiavello, D. Gerace, and D. Bajoni, “An artificial neuron implemented on an actual quantum processor,” *npj Quantum Information* **5**, 1 (2019).
- [82] I. Cong and L. Duan, “Quantum discriminant analysis for dimensionality reduction and classification,” *New Journal of Physics* **18**, 073011 (2016).
- [83] I. Kerenidis and A. Prakash, “Quantum recommendation systems,” in *8th Innovations in Theoretical Computer Science Conference (ITCS 2017)* (Schloss Dagstuhl-Leibniz-Zentrum fuer Informatik, 2017).
- [84] V. Giovannetti, S. Lloyd, and L. Maccone, “Architectures for a quantum random access memory,” *Phys. Rev. A* **78**, 052310 (2008).
- [85] S. Lloyd, M. Mohseni, and P. Rebentrost, “Quantum algorithms for supervised and unsupervised machine learning,” [arXiv:1307.0411 \(2013\)](#).
- [86] N. Wiebe, A. Kapoor, and K. M. Svore, “Quantum deep learning,” [arXiv:1412.3489 \(2014\)](#).
- [87] V. Giovannetti, S. Lloyd, and L. Maccone, “Quantum random access memory,” *Phys. Rev. Lett.* **100**, 160501 (2008).
- [88] A. Scott, “Read the fine print,” *Nat. Phys.* **11**, 291 (2015).
- [89] M. Möttönen, J. J. Vartiainen, V. Bergholm, and M. M. Salomaa, “Quantum circuits for general multiqubit gates,” *Phys. Rev. Lett* **93**, 130502 (2004).
- [90] E. Knill, “Approximation by quantum circuits,” [arXiv:quant-](#)

- ph/9508006 [quant-ph] (1995).
- [91] M. Plesch and Č. Brukner, “Quantum-state preparation with universal gate decompositions,” *Phys. Rev. A* **83**, 032302 (2011).
- [92] L. Grover and T. Rudolph, “Creating superpositions that correspond to efficiently integrable probability distributions,” [arXiv: quant-ph/0208112\[quant-ph\]](https://arxiv.org/abs/quant-ph/0208112) (2002).
- [93] A. N. Soklakov and R. Schack, “Efficient state preparation for a register of quantum bits,” *Phys. Rev. A* **73**, 012307 (2006).
- [94] F. Wilde, R. Sweke, J. Meyer, M. Schuld, P. Fährmann, B. Meynard-Piganeau, and J. Eisert, “Stochastic gradient descent for hybrid quantum-classical optimization,” *Bulletin of the American Physical Society* **65** (2020).
- [95] N. Yamamoto, “On the natural gradient for variational quantum eigensolver,” [arXiv:1909.05074](https://arxiv.org/abs/1909.05074) (2019).
- [96] J. Stokes, J. Izaac, N. Killoran, and G. Carleo, “Quantum natural gradient,” [arXiv:1909.02108](https://arxiv.org/abs/1909.02108) (2019).
- [97] D. P. Kingma and J. Ba, “Adam: A method for stochastic optimization,” [arXiv:1412.6980](https://arxiv.org/abs/1412.6980) (2014).
- [98] J. R. Sashank, K. Satyen, and K. Sanjiv, “On the convergence of adam and beyond,” in *6th International Conference on Learning Representations, ICLR 2018, Vancouver, BC, Canada, April 30 - May 3, 2018, Conference Track Proceedings* (2018).
- [99] J.-G. Liu and L. Wang, “Differentiable learning of quantum circuit born machines,” *Phys. Rev. A* **98**, 062324 (2018).
- [100] A. Harrow and J. Napp, “Low-depth gradient measurements can improve convergence in variational hybrid quantum-classical algorithms,” [arXiv:1901.05374](https://arxiv.org/abs/1901.05374) (2019).
- [101] “<https://github.com/quantumfbs/yao.jl>,” .
- [102] J. Bezanson, A. Edelman, S. Karpinski, and V. B. Shah, “Julia: A fresh approach to numerical computing,” *SIAM review* **59**, 65 (2017).
- [103] “<https://github.com/quantumfbs/cuyao.jl>,” .
- [104] M. Innes, “Flux: Elegant machine learning with julia,” *Journal of Open Source Software* **3**, 602 (2018).
- [105] “<https://github.com/fluxml/zygote.jl>,” .
- [106] N. Srivastava, G. Hinton, A. Krizhevsky, I. Sutskever, and R. Salakhutdinov, “Dropout: a simple way to prevent neural networks from overfitting,” *The journal of machine learning research* **15**, 1929 (2014).
- [107] L. B. Rall and G. F. Corliss, “An introduction to automatic differentiation,” *Computational Differentiation: Techniques, Applications, and Tools* **89** (1996).
- [108] N. Papernot, P. McDaniel, and I. Goodfellow, “Transferability in machine learning: from phenomena to black-box attacks using adversarial samples,” [arXiv:1605.07277](https://arxiv.org/abs/1605.07277) (2016).
- [109] N. Papernot, P. McDaniel, I. Goodfellow, S. Jha, Z. B. Celik, and A. Swami, “Practical black-box attacks against machine learning,” in *Proceedings of the 2017 ACM on Asia conference on computer and communications security* (2017) pp. 506–519.
- [110] F. Tramèr, F. Zhang, A. Juels, M. K. Reiter, and T. Ristenpart, “Stealing machine learning models via prediction apis,” in *25th {USENIX} Security Symposium ({USENIX} Security 16)* (2016) pp. 601–618.
- [111] M. Fredrikson, S. Jha, and T. Ristenpart, “Model inversion attacks that exploit confidence information and basic countermeasures,” in *Proceedings of the 22nd ACM SIGSAC Conference on Computer and Communications Security* (2015) pp. 1322–1333.
- [112] I. Rosenberg, A. Shabtai, L. Rokach, and Y. Elovici, “Generic black-box end-to-end attack against rnns and other api calls based malware classifiers,” [arXiv:1707.05970](https://arxiv.org/abs/1707.05970) (2017).
- [113] B. Hitaj, G. Ateniese, and F. Perez-Cruz, “Deep models under the gan: information leakage from collaborative deep learning,” in *Proceedings of the 2017 ACM SIGSAC Conference on Computer and Communications Security* (2017) pp. 603–618.

Supplementary Material for: Universal Adversarial Examples and Perturbations for Quantum Classifiers

In this Supplementary Material, we provide more details about the proofs of the two theorems, structures of the quantum classifiers, quantum encoding for classical data, training and attacking processes, and the algorithms for obtaining universal adversarial examples and perturbations.

A. PROOF FOR THEOREM 1

In addition to the ones in the main text, we first give more notations and definitions to formulate the problem.

Definition A1. For $\mathcal{H}' \subseteq \mathcal{H}$, we define the *concentration function* as $\alpha(\epsilon) = 1 - \inf\{\mu(\mathcal{H}') | \mu(\mathcal{H}) \geq \frac{1}{2}\}$ with distance measure $D(\cdot)$ and probability measure $\mu(\cdot)$ in a d -dimensional vector space. If

$$\alpha(\epsilon) \leq \alpha e^{-\beta \epsilon^2 d}, \quad (\text{S1})$$

then the vector space is said to be in (α, β) -normal Levy group.

We also introduce the following Lemma A1, which has already been obtained in Ref. [41]. Here, we recap the statement and sketch the proof for completeness.

Lemma A1. For a quantum classifier \mathcal{C}_i that takes $\rho \in SU(d)$ according to the Haar measure $\mu(\cdot)$ as input and has a misclassified set \mathcal{E}_i . Suppose the adversarial input state ρ' is restricted by $d_{HS}(\rho, \rho') \leq \epsilon$ to the clean data ρ . Then to guarantee an adversarial risk R_i , ϵ is bounded below by

$$\epsilon^2 \geq \frac{4}{d} \ln \left[\frac{2}{\mu(\mathcal{E}_i)(1 - R_i)} \right]. \quad (\text{S2})$$

To prove Lemma A1, we further introduce the following two lemmas together with their brief proofs.

Lemma A2. (Theorem 3.7 in [52]) For each classifiers \mathcal{C}_i and risk $\mu(\mathcal{E}_i)$, consider additional perturbation $\rho \rightarrow \rho'$, $\rho, \rho' \in \mathcal{H}$ and $D(\rho, \rho') \leq \epsilon$. If the adversarial risk $\mu(\mathcal{E}_{i,\epsilon})$ is guaranteed to be at least R_i , then ϵ^2 must also be bounded by

$$\epsilon^2 \geq \frac{1}{\beta d} \ln \left[\frac{\alpha^2}{\mu(\mathcal{E}_i)(1 - R_i)} \right]. \quad (\text{S3})$$

Proof. We decompose the perturbation $\epsilon = \epsilon_1 + \epsilon_2$. First construct a ϵ_1 such that $\mu(\mathcal{E}_i) > \alpha e^{-\beta \epsilon_1^2 d}$. Consider two cases for whether $\mu(\mathcal{E}_i) \leq \frac{1}{2}$.

(i) If $\mu(\mathcal{E}_i) > \frac{1}{2}$, then we have $\mu(\mathcal{E}_{i,\epsilon_1}) > \mu(\mathcal{E}_i) > \frac{1}{2}$.

(ii) If $\mu(\mathcal{E}_i) \leq \frac{1}{2}$, suppose $\mu(\mathcal{E}_{i,\epsilon_1}) \leq \frac{1}{2}$. Then the complement probability $\mu(\mathcal{H} \setminus \mathcal{E}_{i,\epsilon_1}) \geq \frac{1}{2}$. Denote $\mathcal{H}'_i = \mathcal{H} \setminus \mathcal{E}_{i,\epsilon_1}$, then $\mu(\mathcal{H}'_i) \geq \frac{1}{2}$ and $\mathcal{E}_i = \mathcal{H} \setminus \mathcal{H}'_{i,\epsilon_1}$. Hence, we can deduce a contradiction using (S1) as $\alpha(\epsilon_1) \geq 1 - \mu(\mathcal{H}'_{i,\epsilon_1}) = \mu(\mathcal{E}_i) > \alpha(\epsilon_1)$.

Therefore, the perturbation ϵ_1 ensures $\mu(\mathcal{E}_{i,\epsilon_1}) > \frac{1}{2}$. Then we attach ϵ_2 to $\mathcal{E}_{i,\epsilon_1}$, which is $\epsilon = \epsilon_1 + \epsilon_2$ perturbation on \mathcal{E}_i .

Applying (S1) we can prove the lemma as $R_i = \mu(\mathcal{E}_{i,\epsilon}) = \mu(\mathcal{E}_{i,\epsilon_1+\epsilon_2}) > 1 - \alpha(\epsilon_2)$ and $\epsilon^2 < \epsilon_1^2 + \epsilon_2^2 = \frac{1}{\beta d} \left\{ \ln \left[\frac{\alpha}{\mu(\mathcal{E}_i)} \right] + \ln \frac{\alpha}{(1-R_i)} \right\}$.

Lemma A3. $SU(d)$ group with Haar probability measure and normalized Hilbert-Schmidt metric is in $(\sqrt{2}, \frac{1}{4})$ -normal Levy group [63, 64].

Proof. First apply isoperimetric inequality [63, 65], which states that for $\mathcal{H}' \subseteq \mathcal{H}$, $\dim(\mathcal{H}) = d$ and $\mu(\mathcal{H}') \geq \frac{1}{2}$,

$$\mu(\mathcal{H}'_\epsilon) \geq 1 - \sqrt{2} e^{-\epsilon^2 d R(\mathcal{H}) / [2(d-1)]}, \quad (\text{S4})$$

where $R(\mathcal{H}) = \inf_v \text{Ric}(v, v)$ for the Ricci curvature $\text{Ric}(v, v')$ of \mathcal{H} and v goes through all unit tangent vectors in \mathcal{H} . Combining (S4) and (S1) we can deduce that

$$\alpha(\epsilon) \leq \sqrt{2} e^{-\epsilon^2 d R(\mathcal{H}) / 2(d-1)}. \quad (\text{S5})$$

According to [66], for $SU(d)$ equipped with Hilbert-Schmidt metric, $\text{Ric}(v, v) = \frac{d}{2} G(v, v)$. And $G(v, v)$ is the Hilbert-Schmidt metric and v is any unit tangent vector in $SU(d)$. Then from [67] $G(v, v) = 1$. Therefore, $R(\mathcal{H}) = \frac{d}{2}$. This indicates that we can rewrite (S5) as

$$\alpha(\epsilon) \leq \sqrt{2} e^{-\epsilon^2 d^2 / 4(d-1)} < \sqrt{2} e^{-\epsilon^2 d / 4}. \quad (\text{S6})$$

Combining (S3) and (S6), it is shown that for a classifier \mathcal{C}_i with risk \mathcal{E}_i which takes $\rho \in SU(d)$ as input and the Hilbert-Schmidt metric, to bound above adversarial risk with R_i , the adversarial perturbation is bounded below by $\epsilon^2 \geq \frac{4}{d} \ln \left[\frac{2}{\mu(\mathcal{E}_i)(1-R_i)} \right]$. Hence, we have completed the proof for Lemma A1.

Now, we continue to prove the Theorem 1 in the main text by using the Ineq. (S2). We consider a set of quantum classifiers \mathcal{C}_i , $i = 1, \dots, k$ with risk \mathcal{E}_i , $i = 1, \dots, k$. Our goal is to calculate $\mu(\mathcal{E}_\epsilon)$ for a given ϵ perturbation. Consider the set $\mathcal{E}_{\text{set}} = \cap_{i=1}^k \mathcal{E}_i$ of original data that is misclassified by all classifiers in the set. If we assume an additional condition $\mathcal{E}_{\text{set}} \neq \emptyset$, then we can construct a quantum classifier \mathcal{C}^* that misclassifies all $\rho \in \mathcal{E}_{\text{set}}$ and correctly classifies other states in \mathcal{H} . Then we apply (S2) to this classifier \mathcal{C}^* and can deduce that to guarantee a risk larger than R_0 , the perturbation is bounded below by

$$\epsilon^2 \geq \frac{4}{d} \ln \left[\frac{2}{\mu(\mathcal{E}_{\text{set}})(1 - R_0)} \right]. \quad (\text{S7})$$

If the additional constraint is not satisfied, i.e. $\cap_{i=1}^k \mathcal{E}_i = \emptyset$, then we can not directly construct a quantum classifier \mathcal{C}^* . In this case, we notice that $\mathcal{E}_\epsilon = \cap_{i=1}^k \mathcal{E}_{i,\epsilon} = \mathcal{H} \setminus \cup_{i=1}^k (\mathcal{H} \setminus \mathcal{E}_{i,\epsilon})$. Therefore $\mu(\mathcal{E}_\epsilon)$ can be bounded below by:

$$\mu(\mathcal{E}_\epsilon) \geq 1 - \sum_{i=1}^k \frac{|\mathcal{H} \setminus \mathcal{E}_{i,\epsilon}|}{|\mathcal{H}|} = \sum_{i=1}^k \mu(\mathcal{E}_{i,\epsilon}) - (k-1). \quad (\text{S8})$$

Hence, if we attach a perturbation that ensures $\mu(\mathcal{E}_{i,\epsilon}) \geq R_{0,i} = \frac{k-1+R}{k}$ for each classifier \mathcal{C}_i , then the universal adversarial risk will be bounded below by R . Replacing R and

$\mu(\mathcal{E}_i)$ in (S2) with R_0 and $\mu(\mathcal{E})_{\min}$, we finish the proof by arriving at the inequality:

$$\epsilon^2 \geq \frac{4}{d} \ln \left[\frac{2k}{\mu(\mathcal{E})_{\min}(1 - R_0)} \right]. \quad (\text{S9})$$

It is worthwhile to mention that the Ineq. (S9) holds regardless of whether the additional assumption $\mathcal{E}_{\text{set}} \neq \emptyset$ is satisfied or not. When $\mathcal{E}_{\text{set}} \neq \emptyset$ is satisfied, the problem reduces to the case for the single classifier C^* . Yet, we cannot tell which inequality, either Ineq. (S7) or (S9), gives a tighter bound as we have no information about the value of $\mu(\mathcal{E}_{\text{set}})$ and $\mu(\mathcal{E}_{\min})$. In our numerical simulations, among the test set containing 100 ground states of the Ising model, we find that there are five samples that can be misclassified by all eight quantum classifiers without adding any perturbation. This indicates that the additional condition might be satisfied in practice.

B. PROOF FOR THEOREM 2

In this section, we provide the details of the proof for Theorem 2 with some further discussions. Following the definitions in the main text, the adversarial operator $\hat{\epsilon}$ is unitary, and hence $\hat{\epsilon}^{-1}$ is also unitary. Then by applying the property of unitary transformation, we have

$$\mu(\mathcal{E}_{\hat{\epsilon}}) = \frac{|\hat{\epsilon}^{-1}(\mathcal{E})|}{|\mathcal{H}|} = \frac{|\mathcal{E}|}{|\mathcal{H}|} = \mu(\mathcal{E}). \quad (\text{S10})$$

This indicates that the adversarial risk remains the same after we perform the same unitary perturbation operation $\hat{\epsilon}$ on every input quantum state $\rho \in \mathcal{H}$.

We randomly pick $\rho \in \mathcal{H}$ according to the Haar measure. For each selection, the probability of misclassification occurrence is $\mu(\mathcal{E}_{\hat{\epsilon}}) = \mu(\mathcal{E})$. Therefore, we can regard each selection as a random variable, which will be 1 when misclassification occurs and 0 otherwise. Then, we apply Hoeffding's inequality for independent Bernoulli random variables and get with probability at least $1 - \delta$ ($\delta > 0$)

$$|R_E - \mu(\mathcal{E})| \leq \sqrt{\frac{1}{2n} \ln \left(\frac{2}{\delta} \right)}. \quad (\text{S11})$$

This proves the first part of the Theorem 2 in the main text.

To obtain an lower bound for $\mu(\mathcal{E})$, we further resort to the no free lunch theorem [59] and its reformulation in the context of quantum machine learning [47, 48]. Unlike in Ref. [47], where quantum input and output are considered, our discussion is restricted to classification problems in which the output is classical labels. To this end, here we give a loose estimation for the lower bound of $\mu(\mathcal{E})$ with some additional constraints according to our numerical simulations.

In our consideration, the quantum classifiers takes two steps to classify input samples. In the first step, the classifier takes a quantum state $\rho \in \mathcal{H}$ as input and undergoes a variational circuit to arrive at the output state ρ_{out} belonging to a d' -dimensional Hilbert space. In the second step, the classifier

outputs a label $s \in \{0, 1, \dots, d' - 1\}$ according to the largest probability among $\langle 0 | \rho_{\text{out}} | 0 \rangle, \langle 1 | \rho_{\text{out}} | 1 \rangle, \dots, \langle d' - 1 | \rho_{\text{out}} | d' - 1 \rangle$. Based on this, our analysis of $\mu(\mathcal{E})$ will lead to an average performance bound for the classifier [47].

In the first step from ρ to ρ_{out} , the quantum ground truth is defined as a unitary process t . Without loss of generality, we may restrict our discussion to the case of quantum pure states. The training set is rewritten as $\mathcal{S}_N = \{(|\psi_1\rangle, |\phi_1\rangle), \dots, (|\psi_N\rangle, |\phi_N\rangle)\}$ and the classifier learns a hypothesis operator V , which is a unitary process such that $t|\psi_i\rangle = V|\psi_i\rangle = |\phi_i\rangle$ for the training set. The quantum risk function is defined as [68].

$$R_t(V) \equiv \int d|\psi\rangle ||t|\psi\rangle\langle\psi|t^\dagger - V|\psi\rangle\langle\psi|V^\dagger||_1^2, \quad (\text{S12})$$

where $||A||_1$ is the trace norm for matrices [6]. Now the quantum no free lunch theorem is described as below.

Lemma B1. (Quantum No Free Lunch) The quantum risk function in a classification task averaged over selection of quantum ground truth t and training set \mathcal{S}_N with respect to the Haar measure can be bounded below by

$$\mathbb{E}_t[\mathbb{E}_{\mathcal{S}_N}[R_t(V)]] \geq 1 - \frac{1}{d(d+1)}(N^2 + d + 1). \quad (\text{S13})$$

The proof of this lemma and more discussions about its implications are provided in Refs. [47, 48]. Here, we use this lemma to obtain Ineq. (4) in the main text. Noting that $||A||_1 \leq 1$, hence for all the $\rho = |\psi\rangle\langle\psi| \in \mathcal{E}$, $D(t|\psi\rangle, V|\psi\rangle) = ||t|\psi\rangle\langle\psi|t^\dagger - V|\psi\rangle\langle\psi|V^\dagger||_1 \leq 1$. This means that $R_t(V) \leq 1$, regardless of whether the quantum data is correctly classified or not.

Then we come to the case when a quantum input is classified correctly. Without loss of generality, we can assume that the ground truth gives true label and output state $t|\psi\rangle = |i\rangle$, then since the quantum data is correctly predicted, $\langle i | t|\psi\rangle\langle\psi|t^\dagger | i \rangle \geq \frac{1}{d'}$. From this inequality, we obtain that the fidelity $F(V|\psi\rangle, t|\psi\rangle = |i\rangle) \geq \sqrt{\frac{1}{d'}}$. We can utilize the relation between fidelity and the trace norm

$$D(\rho, \sigma)^2 \leq 1 - F(\rho, \sigma)^2, \quad (\text{S14})$$

where ρ, σ denote arbitrary quantum states.

Hence, for correctly classified quantum data we have $R_t(V) = D(t|\psi\rangle, V|\psi\rangle)^2 = ||t|\psi\rangle\langle\psi|t^\dagger - V|\psi\rangle\langle\psi|V^\dagger||_1^2 \leq 1 - F(t|\psi\rangle, V|\psi\rangle)^2 \leq 1 - \frac{1}{d'}$. As a result, the integral in Eq. (S12) is bounded by

$$R_t(V) \leq \mu(\mathcal{E}) + \frac{d' - 1}{d'}(1 - \mu(\mathcal{E})) = \frac{1}{d'}(d' - 1 + \mu(\mathcal{E})). \quad (\text{S15})$$

Combining (S13) and (S15), we obtain a lower bound of $\mu(\mathcal{E})$ averaged over ground truth t and training set \mathcal{S}_N

$$\mathbb{E}_t[\mathbb{E}_{\mathcal{S}_N}[\mu(\mathcal{E})]] \geq 1 - \frac{d'}{d(d+1)}(N^2 + d + 1). \quad (\text{S16})$$

This gives the Ineq. (4) and complete the proof of Theorem 2.

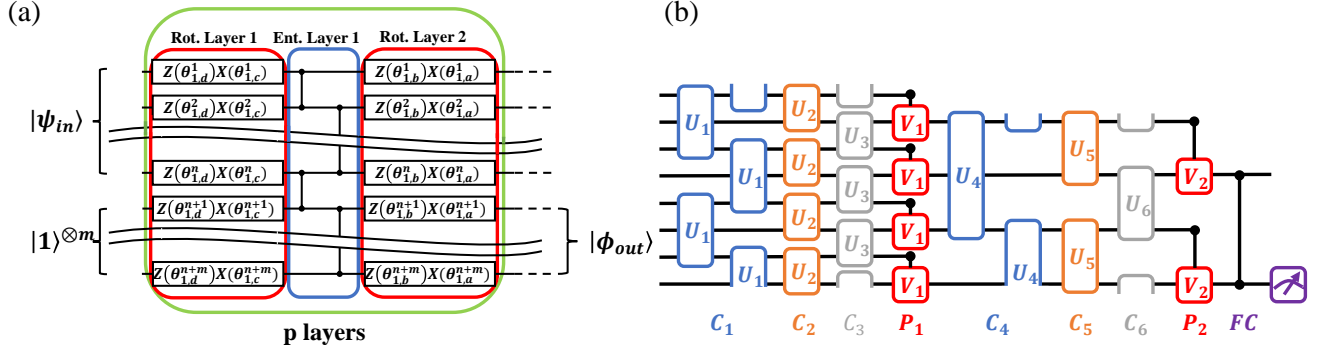


FIG. S1: The structure of quantum classifiers used in the numerical simulations. (a) The illustrative structure of a general multi-layer quantum variational classifier that takes n -qubit state $|\psi_{in}\rangle$ as input and outputs a m -qubit state $|\phi_{out}\rangle$. The classifier consists of p layers and each layer consists two rotation units and an entangler unit. Each rotation unit contains a Euler rotation $Z(\theta_{i,u}^k)X(\theta_{i,v}^k)$ [$(u, v) = (d, c)$ or (b, a)], where $i = 1, \dots, p$ refer to the number of layers, $k = 1, \dots, m + n$ denote the number of qubit. After obtaining the output state $|\phi_{out}\rangle$, we compute the probabilities of projection measurements to predict and assign a label that corresponds to the largest probability. (b) The illustrative structure of the QCNN classifier. This circuit contains six convolutional layers labeled by C_1 to C_6 , two polling layers labeled by P_1 and P_2 respectively, and a fully connected layer labeled by FC . The initial parameters are set to random values at the beginning of the training process.

C. THE STRUCTURES OF QUANTUM CLASSIFIERS AND ENCODING METHODS

I. The structures of quantum classifiers

In recent years, a number of different quantum classifiers have been proposed [34, 35, 54, 69–81]. Here, we choose some of these classifiers to form the classifier set considered in this paper. As mentioned in the main text, our classifier set contains two QCNNs [54] and six general multi-layer variational classifiers [69, 70, 72, 73]. The sketch of a quantum variational circuit is shown in Fig. S1(a).

In such a variational circuit model, we first prepare the $m + n$ qubit input state to be $|\psi_{in}\rangle \otimes |1\rangle^{\otimes m}$, where $|\psi_{in}\rangle$ is an n -qubit state that encodes the complete information of input sample to be classified. Then we apply a unitary transformation, which is composed of p layers of interleaved operations, on the state. In each of the p layers, there are two rotation units each performs arbitrary Euler rotations in Bloch sphere and an entangler unit consisting of CNOT gates between each pair of neighboring qubits. The adjustable parameters are the rotation angles and are collectively denoted as Θ . This generates a variational state:

$$|\Phi(\Theta)\rangle = \prod_{i=1}^p U_i(|\psi_{in}\rangle \otimes |1\rangle^{\otimes m}), \quad (\text{S17})$$

where $U_i = \prod_k Z(\theta_{i,d}^k)X(\theta_{i,c}^k)U_{\text{ent}}Z(\theta_{i,b}^k)X(\theta_{i,a}^k)$ denotes the unitary operation for the i -th layer, with U_{ent} representing the unitary operation generated by the entangler unit.

The brief structure of the QCNN and its hyperparameters utilized in this paper is shown in Fig. S1(b). The structure of the QCNN is the same as in Ref. [54].

In our numerical simulations, we only focus on two-category classification problems. Thus, we only need one

qubit to encode the labels $y = 0, 1$. After the variational circuits, the state of the output qubits becomes ρ_{out} . We compute $\mathbb{P}(y = m) = \text{Tr}(\rho_{out}|m\rangle\langle m|)$ and then assign $y = 1$ if $P(y = 1) \geq P(y = 0)$ and $y = 0$ for other cases.

II. Quantum encoding for classical data

In the main text, one of the numerical simulations we did is based on the images of handwritten digits. In this dataset, the images are encoded classically, i.e. the data is encoded into a m -dimensional vector \mathbf{v} in \mathbb{R}^m . To make such classical data processable to quantum classifiers, we need to convert the classic vector into a n -qubit quantum (pure) state in a $d = 2^n$ dimensional Hilbert space. This converting process is called a quantum encoder. In this paper, we use the amplitude encoder to transfer classical data into quantum states [27, 35, 69, 71, 82–88].

For an amplitude encoder, each component of \mathbf{v} is then represented by the amplitude of the n -qubit ket vector $|\psi_{in}\rangle$ represented in computational basis. Without loss of generality, we assume that $m = 2^n$ is a power of 2, otherwise we can attach $2^n - m$ zeros to the end of the vector \mathbf{v} so that it can be transformed into a n qubit pure state. The encoder can be realized by a circuit and the depth of the circuit is linear with the number of features [89–91]. Under certain conditions, a polynomial size of gate complexity over m might be needed [92, 93]. Such encoding procedure can be improved using a more complex approach like tensorial feature maps [69].

III. The training process of quantum classifiers

In classical machine learning, different loss functions are introduced when training the networks and estimating the per-

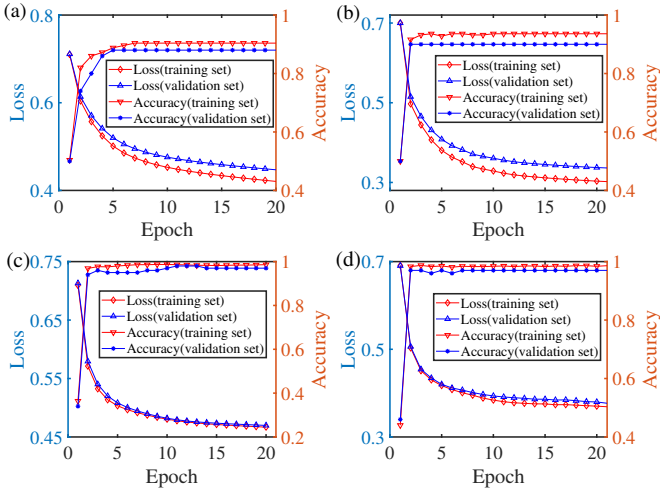


FIG. S2: The average loss and accuracy for quantum classifiers 2 and 8 during the training process, in classifying handwritten digit images and the ground states of the 1D transverse field Ising model. (a) The training procedure of the classifier 2 (a QCNN classifier) for classifying the ground states. Each epoch contains 30 iterations. (b) The training procedure of the classifier 8 with depth $p = 10$ for classifying the ground states. Each epoch contains 5 iterations. (c) The training procedure of the classifier 2 for classifying handwritten digit images. Each epoch contains 50 iterations. (d) The training procedure of classifier 8 for classifying handwritten digit images. Each epoch represents 10 iterations.

formance. In numerical simulations, we employ a quantum version of cross-entropy as

$$\mathcal{L}(h(|\psi\rangle; \Theta), \mathbf{p}) = - \sum_{k=1}^2 p_k \log q_k, \quad (\text{S18})$$

where $\mathbf{q} = (q_1, q_2)$ is the diagonalized expression of output state $\text{diag}(\rho_{\text{out}})$ and $\mathbf{p} = (1, 0)$ for $y = 0$ and $\mathbf{p} = (0, 1)$ for $y = 1$. In the training procedure of a quantum classifier, an optimizer is used to adjust the parameter Θ to minimize the empirical loss function $\mathcal{L}_N(\theta) = \frac{1}{N} \sum_{i=1}^N \mathcal{L}(h(|\psi_i\rangle; \Theta), \mathbf{p}_i)$. In recent years, a large family of gradient-based algorithms have been broadly used in training classical and quantum neural networks[94–98]. In the numerical simulations in this research, we use Adam optimization algorithm [97, 98], which is a gradient-based learning algorithm with adaptive learning rate.

To find the minimization of the loss function using multiple-step gradient-based methods, we need to calculate the gradient of $\mathcal{L}_N(\Theta)$ over parameter Θ . Each component of the gradient is represented as $\frac{\partial \mathcal{L}_N(\Theta)_\theta}{\partial \theta} = \lim_{\epsilon \rightarrow 0} \frac{1}{2\epsilon} [\mathcal{L}_N(\Theta)_{\theta+\epsilon} - \mathcal{L}_N(\Theta)_{\theta-\epsilon}]$ where θ is one of the parameters of Θ . Owing to the special structures of the quantum classifiers, we use the “parameter shift rule” [40, 99, 100] in our numerical simulations to obtain the gradients required.

In Fig. S2, we plot the average loss and accuracy of some of quantum classifiers in our classifier set during the training procedure. The numerical simulations including the train-

ing procedure and adversarial attack were done on a classical cluster using Yao.jl[101] and its extension packages in Julia language[102]. To run the simulation on GPU, i.e. to perfectly fit the mini-batch gradient descent algorithm, we use CuYao.jl[103]. This package is an efficient extension of Yao.jl on GPU calculation that can obtain a speedup. Flux.jl[104] and Zygote.jl[105] packages are used to calculate the differentiation of the function. We note that the overfitting risk is low as the loss of the training data and validation data is close.[106].

In Table S1, we list the number of parameters for each quantum classifier used in this paper, and their final accuracy in classifying the ground states of the 1D transverse field Ising model.

Classifier	Structure	Number of parameters	Accuracy
1	QCNN	44	0.917
2	QCNN	92	0.950
3	Variational Circuit	144	0.923
4	Variational Circuit	171	0.930
5	Variational Circuit	198	0.940
6	Variational Circuit	225	0.930
7	Variational Circuit	252	0.947
8	Variational Circuit	279	0.955

TABLE S1: The number of parameters and the final accuracy after the training process for each quantum classifier in classifying the ground states of the 1D Ising model. The accuracy is calculated over a training set that contains 300 samples.

D. ADVERSARIAL ALGORITHMS

In this section, we provide more details on the algorithms for obtaining adversarial examples and perturbations.

When proposing an adversarial attack on a quantum classifier that takes quantum data as input, we maximize the adversarial risk $\mu(\mathcal{E})$ mentioned in the main text. However, in practice $\mu(\mathcal{E})$ is typically inaccessible. Hence, we consider maximizing the loss function instead. It is worthwhile to mention that a maximal loss function value does not always indicates a maximal risk. In the quantum scenario, we denote the adversarial perturbation attached to the quantum sample as an operator U_δ that acts on the input state. The maximization problem of adding perturbation can be described as:

$$U_\delta \equiv \arg \max_{U_\delta \in \Delta} \mathcal{L}(h(U_\delta|\psi\rangle; \Theta^*), \mathbf{p}), \quad (\text{S19})$$

where Θ^* denotes the optimized parameters after the training process, Δ are the possible perturbations that can be added, $|\psi\rangle$ is the original input state and \mathbf{p} is the correct label. In the case of studying universal adversarial examples, we have a test set $\mathcal{T}_M = \{(|\psi_0\rangle, y_0), \dots, (|\psi_M\rangle, y_M)\}$ and a set of quantum classifiers which learn hypothesis functions h_1, h_2, \dots, h_k . In order to obtain universal adversarial examples that can deceive all the quantum classifiers in the set, we solve the following

optimization problem:

$$U_\delta^j \equiv \arg \max_{U_\delta^j \in \Delta} \sum_{i=1}^k \mathcal{L}(h_i(U_\delta^j |\psi_j); \Theta^*, \mathbf{p}_j), \quad (\text{S20})$$

where U_δ^j is the perturbation for the j -th sample. For the case of obtaining universal adversarial perturbations, we use an identical perturbation to implement the adversarial attack to all samples in the test set \mathcal{T}_M . In this case, we have one quantum classifier and its hypothesis function h . The maximization problem can be expressed in the similar form

$$U_\delta \equiv \arg \max_{U_\delta \in \Delta} \frac{1}{M} \sum_{i=1}^M \mathcal{L}(h(U_\delta |\psi_i); \Theta^*, \mathbf{p}_i). \quad (\text{S21})$$

In general, the set Δ can be the set of unitary operators that are close to the identity matrix. We use automatic differentiation [107] to improve precision when applying the perturbation. In practice, we restrict the set Δ to be the product of local unitary operators near the identity matrix.

In the white-box attack scenario, the attacker has the full information of the classifiers, including their inner structures and loss functions. The attacker can then calculate the gradient of loss functions $\nabla \mathcal{L}(h(|\psi\rangle; \Theta^*, \mathbf{p}))$. In this scenario,

we use the quantum-adapted Basic Iterative Method (qBIM) introduced in Ref. [40] to solve the above optimization problems in Eq. (S20) and (S21).

Compared with a white-box scenario, the adversary in a black-box setting does not have complete information of the quantum classifier. In classical adversarial learning, the development of black-box assumption has been divided into several categories. In non-adaptive black-box attack [108–110], the adversary knows nothing about the classifier’s inner structure but can get access to the training data and analyze its distribution. In adaptive black-box scenario [109, 111, 112], the attacker can use the classifier as an oracle without extra information provided. Another category is the strict black-box scenario [113], where the data distribution is unknown but the adversary can collect the input-output pairs from the target classifier. In our simulations, we implement the non-adaptive black-box adversarial attack in which we try to use the knowledge of one quantum classifier to attack all quantum classifiers in the set that share the same training set and test set. The result shown in Fig. 2(c) in the main text indicates the effectiveness of such a black-box attack.